Research on ridge buckle of high accuracy cold rolled thin strip at local high points during the coiling process

W.Q. Sun, X.Y. Zhang, A.R. He, J. Shao

Small, narrow waves accompany ridge buckle after a thin strip is uncoiled. The two reasons for this can be judged as: 1) The existence of local small waves after a strip has been cold rolled; 2) Longitudinal deformation due to a second buckling after local high point superposition during the coiling process. The phenomenon presents as a narrow wave shape after the strip is uncoiled. Based on the fundamental theory of elastic mechanics in analyzing the relation between local high points and ridge buckle during the coiling process, this article sets up a three-dimensional model for the coiling process through ANSYS/LS-DYNA Finite Element software. This model simulates well the appearance of local high points during coiling, and the Finite Element model for coiling can truly reflect deformation due to force in the coiling process of a strip. This article also analyzes the changes to local high points during the coiling process, and the dependent variable of the second buckling on a strip, caused by different local high points. A control range is then found of local high points for strips of different thicknesses; in order to reduce the generation of local plastic deformation, and to indicate the forming mechanism of the second ridge buckle after rib point stress superposition during the coiling process. The article provides theoretical and data support for the control of ridge-buckle and ridge buckle on high accuracy cold rolled thin strip during the coiling process.

KEYWORDS: COLD ROLLING - COILING - RIDGE-BUCKLE - ANSYS FEM

INTRODUCTION

A ‘ridge buckle’ defect refers to a ‘bulge’ that appears on a coil surface. This is due to the accumulation, by layer, of local features; including a local thickness high point and local wave shapes, as well as an uneven distribution of local residual stress and other features acting during the coiling process. Ridge buckle, as shown in Fig. 1, is particularly prominent on a thin strip and greatly affects the quality of high precision cold rolled strip. If there are a large number of ridge buckles, an additional small wave shape will appear after the coil has been uncoiled, as shown in Fig. 2 and Fig. 3. This has a serious impact on product performance and appearance; resulting in degradation and scrap of the products[1]. Theoretical study of ridge buckle has mainly been based around using the theory of elasticity to calculate the amount of local ridge buckles. However, this does not explain the formation of waves of ridge buckle on a strip during uncoiling. Melfo, Zhu and other scholars have studied the microstructural and temperature features of hot strips that may lead to ridge-buckle defects in thin-rolled steel strip [2-5]. Zhen Hua supposes that waves are present before coiling and calculates the amount of ridge buckles after the coiling of local waves [6]. In practice though, when the amount of ridge buckles of a strip reaches a certain value, secondary buckling plastic deformation will occur when coiling and will cause waves when uncoiling. Ovesy and Ghannadpour researched the buckling and post-buckling behaviour of moderately thick plates using an exact finite strip[7,8]. Bush, Fischer and Rammerstorfer studied the residual stresses and stress levels that lead to waves and buckling in rolled strip [9-11]. At present, there is little relevant literature on ridge buckles. However, the occurrence frequency of such a phenomenon is high in production and acts as an important factor affecting strip quality. Solving the ridge buckle problem

W.Q.Sun, A.R.He, J.Shao
National Engineering Research Center for Advanced Rolling Technology, University of Science and Technology Beijing, Beijing 100083, China

X.Y.Zhang
Changchun Aviation Hydraulic Control Co., Ltd China, Changchun 130052, China

Corresponding author: W.Q.Sun: wqsun18@163.com

is therefore an important guarantee to improve the market competitiveness of a product. In order to further improve the quality of steel plates and to increase market competitiveness, it is all the more urgent to conduct an in-depth study on the formation mechanism of secondary ridge buckles in the coiling process of strips with ridge buckle.

Fig. 1 - Physical map of a strip with ridge buckle

Fig. 2 - Physical map of ridge buckle after uncoiling of a ridge buckle strip

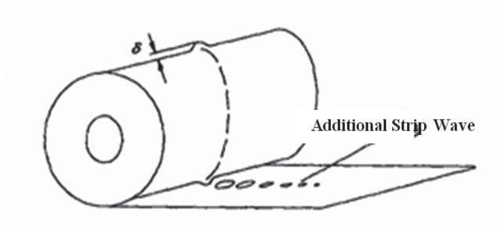

Fig. 3 - Sketch map of ridge buckle after uncoiling of a ridge buckle strip

MEASURED DATA ANALYSIS OF THE FIELD RIDGE BUCKLE COIL PROFILE

From the superficial phenomenon, a ridge buckle is a strip rib that is partially higher than the rest of the strip and which appears when coiling the strip. It is necessary to measure the cold-rolled strip profile, and to then analyze the causes of the ridge buckle. If a ridge buckle is discovered in the process of rolling, production should be suspended for data measurement. The strip of a tandem cold rolling plant is then sampled, both before and after rolling, and the strip profile is measured many times to find the average. The results, shown in Fig. 4 and Fig. 5, demonstrate that there are significant local high points at the part about 100-200mm from the cold plant drive side of the sample, and the local high point cannot be eliminated in the cold rolling process. Due to the local high point, the ridge buckle gradually appears with thickness accumulation. It is clear that the local high points are located between 100-200mm, which coincides with the actual position of the ridge buckle.

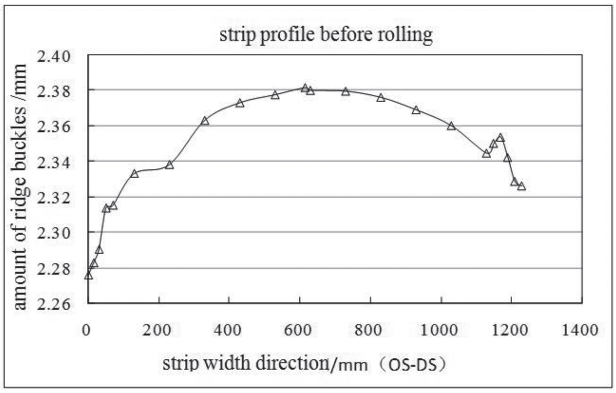

Fig. 4 - Profile of the ridge buckle strip before rolling

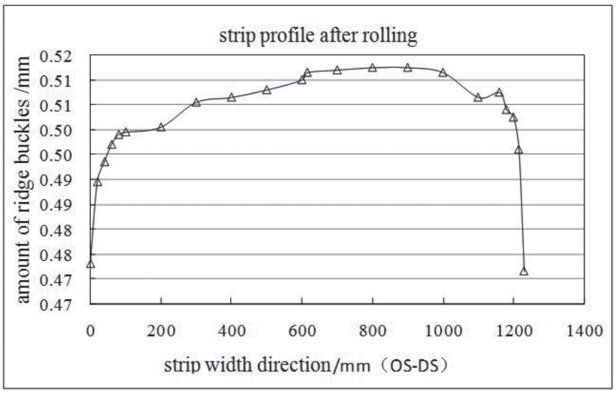

Fig. 5 - Profile of the ridge buckle strip after rolling

By measuring the profile, it can be seen that the main cause of ridge buckles is that there is a local high point on the strip material, which cannot be eliminated in the process of cold rolling process. The strip with a local high point finally develops ridge buckles when coiling; through accumulation by layer. In this case, where the quality of the sample profile must be controlled on the one hand, and on the other hand, the local high point cannot be completely eliminated, it is particularly important to calculate what size of local high point causes plastic deformation to the strip, by calculating the allowable range of the value of local high points.

ANALYTICAL MODEL FOR CALCULATING THE RIDGE BUCKLES

According to the physical model, the stress conditions of the strip and the fact that the strip is coiled on a reel by layer in the practical work of the coiling machine, a mathematical model has been built to calculate the distribution of internal stress in the strip coiling process through accumulation deduction and calculation by layer.

Geometry equation of strip coiling
The stress state of the strip in the coiling process is as shown in Fig. 6; with u representing the displacement along the axis r, and v representing the displacement along the circumferential direction ϑ. According to the theory of elasticity, radial deformation is obtained as follows:

$$\varepsilon_r = \frac{(u + \frac{\partial u}{\partial r}dr) - u}{dr} = \frac{\partial u}{\partial r} \tag{1}$$

$$\varepsilon_\tau = \frac{1}{r} \cdot \frac{\partial v}{\partial \theta} + \frac{u}{r} \tag{2}$$

$$\gamma_{r\tau} = \frac{\partial u}{r \partial \theta} + \frac{\partial v}{\partial r} - \frac{v}{r} \tag{3}$$

The strip coiling process can be considered as an axisymmetric matter. Namely, the strip deformation and stress has nothing to do with the angle.

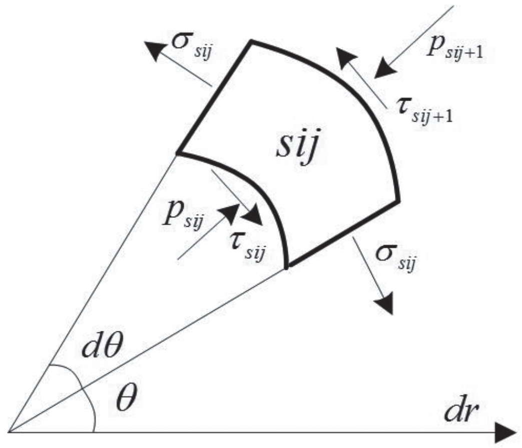

Fig. 6 - Schematic diagram of the coiling strip stress

Physical equation of strip coiling
For the generalized plane stress state, a relationship is built between deformation and the stress of the strip. In a tangential direction, the outer tension of the strip is σ_0, with $\sigma_0 = T_s / bh$. Due to the external pressure on the inner layer, compressive deformation occurs to the inner rings, resulting in disappearance of strip tension [12], so:

$$\sigma_{\tau i} = \sigma_0 - \sigma_i \tag{4}$$

Where σ_i is the actual tension of layer i of the strip among the coiled n layers; $\sigma_{\tau i}$ is the unit tension of layer i.

In the radial direction, besides the usual elastic deflection of the strip during coiling, the effect p_r / E_r of additional deformation is caused when the strip layers touch each other. In this way, the physical equation of the strip is obtained as follows:

$$\begin{cases} \varepsilon_\tau = \frac{1}{E}(\sigma_0 - \sigma_i - \mu p_i) \\ \varepsilon_r = -\frac{\mu}{E}(\sigma_0 - \sigma_i) + m\frac{p_i}{E} \end{cases} \tag{5}$$

Where, E_r is the radial elastic modulus for a steel coil, m is the radial tight coefficient of the strip, and $m = E / E_r$; according to documents [12] and [13], the value of m is measured by the radial laminated plate compression test.

Motion equation of the reel
Change of the strip radius from r to $r + \Delta r$ during the time interval of Δt was analyzed, as shown in Fig. 7. The variation of the total length of the strip is expressed as:

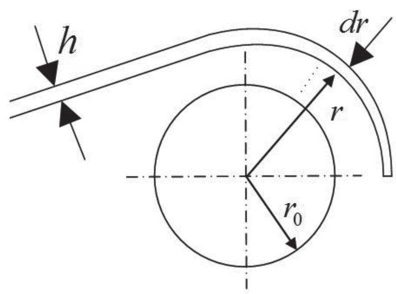

Fig. 7 - Change of the coiling diameter during coiling

$$\Delta s = 2\pi(r + \Delta r) - 2\pi r = 2\pi \Delta r \tag{6}$$

Where Δr is the radial variation of the coiling strip, and with $\Delta r = \varepsilon_r \cdot h$, due to radial deformation of Δr on the outermost layer of the strip, the resulting circumferential displacement of the strip is:

$$\Delta u_i = -2\pi \Delta r \tag{7}$$

According to both the physical and geometrical equations, the outer circumferential displacement of a strip during coiling is:

$$u_\tau = \frac{r}{E}(\sigma_0 - \mu p_r) \tag{8}$$

In this way, an equivalent relationship is built, according to the circumferential deformation of the strip. This finally makes it possible to obtain the interlayer pressure of the outer layer during the strip coiling:

$$p_{ri} = \frac{r_i - 2\pi\mu h}{\mu r_i - 2\pi m h}\sigma_0 \tag{9}$$

Radial equilibrium equation of the strip

As shown in Fig. 7, the friction on both the upper and lower layers of the element body can be equivalent to the circumferential force. By analyzing the radial equilibrium of a single strip element the result is:

$$\left(p_r + dp_r\right)\left(r + dr\right)d\theta - p_r r d\theta = 2\sigma_\tau dr \sin\frac{d\theta}{2} \quad (10)$$

Due to a small $d\theta$, $\sin(d\theta/2) \approx d\theta/2$. By ignoring the infinitely small quantity by three times, however, the radial static equilibrium equation of the strip is:

$$\sigma_\tau + p_r + r\frac{dp_r}{dr} = 0 \quad (11)$$

Here, σ_τ is the equivalent circumferential force. This constitutive equation can be rearranged as follows, after the simultaneous equilibrium and physical equations:

$$\begin{cases} \varepsilon_\tau = \dfrac{1}{E}\left[\sigma_0 + \left(1-\mu\right)p_r + r\dfrac{dp_r}{dr}\right] \\ \varepsilon_r = \dfrac{m}{E}\left[\left(1-\dfrac{\mu}{m}\right)p_r - \dfrac{\mu}{m}\left(\sigma_0 + r\dfrac{dp_r}{dr}\right)\right] \end{cases} \quad (12)$$

Now, it is necessary to calculate the radial stress and deformation of the internal interlayer of the strip. With the tangential strain formula plugged into the formula (2), the circumferential deformation is:

$$u_\tau = \frac{r}{E}\left[\sigma_0 + \left(1-\mu\right)p_r + r\frac{dp_r}{dr}\right] \quad (13)$$

According to the equivalent relationship of the circumferential deformation, the radial pressure formula of the strip inner interlayer when coiling is:

$$p_{ij} = \frac{\left(2\pi\mu r_{ij} + \dfrac{r_{ij}^{\,2}}{h}\right)p_{ij+1} + \left(r_{ij} + 2\pi\mu h\right)\sigma_0}{\left[2\pi\mu h\left(m-\mu\right) + 2\pi\mu r_{ij} + \dfrac{r_{ij}^{\,2}}{h} - r_{ij}\left(1-\mu\right)\right]} \quad (14)$$

Calculation of amount of the strip ridge buckles caused by local high point

According to document [12], the amount of strip ridge buckles of layer k for the strip coiled n layers is expressed as:

$$\Delta_k = h\sum_{i=1}^{k}\left[\frac{\xi\delta}{h}\left(1-\varepsilon_{ri}^{\delta}\right) - \left(\varepsilon_{ri}^{\delta} - \varepsilon_{ri}^{0}\right)\right] \quad (15)$$

Here, ξ is the longitudinal average coefficient of the local high point, and represents the longitudinal change of the local high point along the strip. δ is the value of a local high point; ε_{ri}^{0} is the radial strain of the non-ridge buckle parts; and $\varepsilon_{ri}^{\delta}$ is the radial strain of the ridge buckle parts. $\varepsilon_{ri}^{\delta} \approx 0$, $1-\varepsilon_{ri}^{\delta} \approx 1$, therefore, the formula above can be simplified as:

$$\Delta_k = k(k+1)\xi\delta/2 - h\sum_{i=1}^{k}\left(\varepsilon_{ri}^{\delta} - \varepsilon_{ri}^{0}\right) \quad (16)$$

Obviously, for the formula above, the model introduced previously can be used to calculate ε_{ri}^{0} and $\varepsilon_{ri}^{\delta}$, and to then calculate Δ_k, the amount of ridge buckles, directly.

Analysis of the calculation results of the ridge buckles

Fig. 8 shows the calculation results of the ridge buckles on a strip with a coiling diameter of 1300mm, as related to different local high points when the strip thickness is, respectively, 0.4mm, 0.5mm and 0.6mm. As can be seen, in the case of constant strip thickness, along with the higher value of the local high point, the ridge buckles also increase.

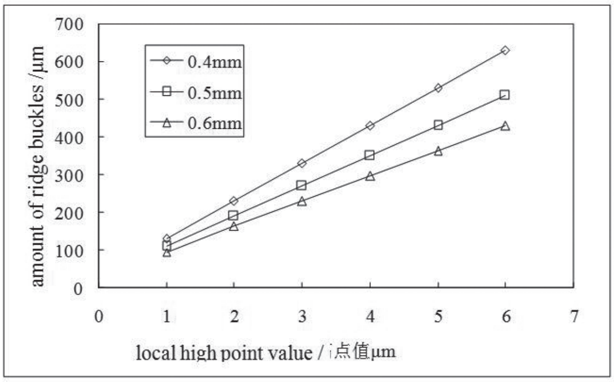

Fig. 8 - Relationship between local high point value and the amount of ridge buckles

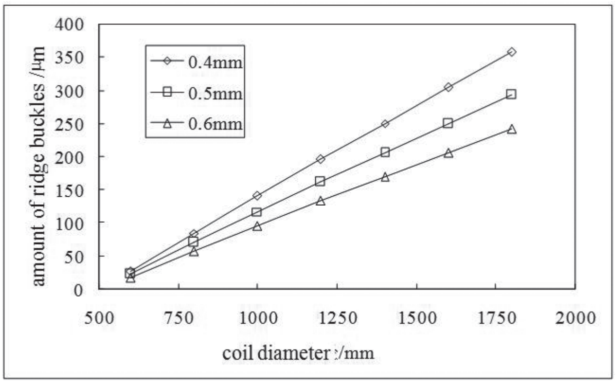

Fig. 9 - Relationship between coil diameter and the amount of ridge buckles

Fig. 9 shows the amount of ridge buckles with a local high point value of 2μm, under different coiling diameters. With the increase of strip size, the quantity of ridge buckles grows. There are also different increase levels for strips with different thicknesses; the thinner the strip is, the higher the increasing speed of the ridge buckles is, for the same local high point value.
Fig. 10 shows the calculation results of ridge buckles with a local high point value of 2μm and a coiling diameter of 1300mm under different coiling tensions. In the case of the constant local high point, as the strip coiling tension increases, the ridge buckles also increase. Within the range of allowed coiling tension, though, the increasing range of the ridge buckles is moderate.

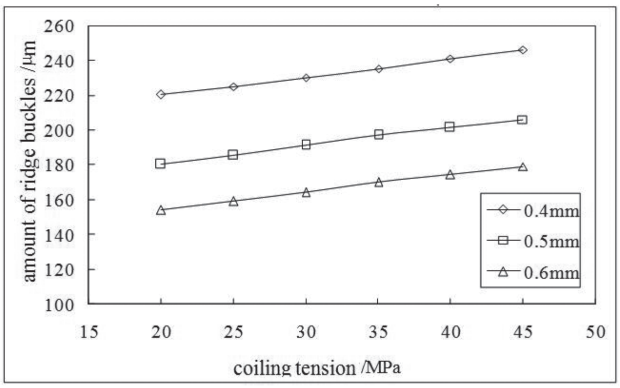

Fig. 10 - Relationship between coiling tension and the amount of ridge buckles

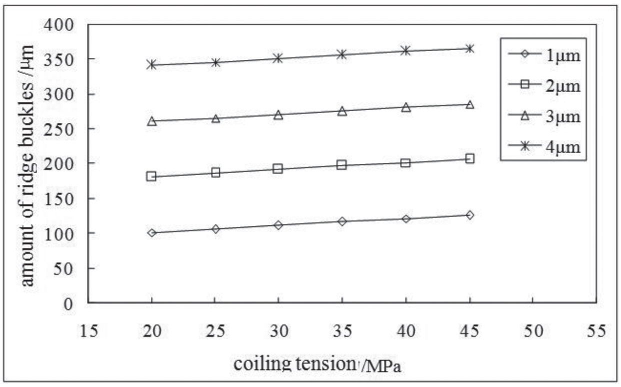

Fig. 11 - Relationship between coiling tension and the amount of ridge buckles

Fig. 11 shows the calculation results of ridge buckles with a strip thickness of 0.5mm, a coiling diameter of 1300mm, and local high points of 1μm, 2μm, 3μm and 4μm respectively, under different coiling tensions. As can be seen, in the case of constant strip thickness, with an increase of strip tension, the increasing range of the ridge buckles is moderate.

FINITE ELEMENT MODEL

Since the above calculation is based on elastic deformation, the amount of strip ridge buckles is linearly related to strip thickness, the value of the local high point, coiling diameter and coiling tension. In order to analyze plastic local deformation occurring in the ridge buckle strip during the coiling process, a finite element model was established for the strip coiling process.

Finite element modeling

For the finite element during coiling, this article will first consider the feasibility of coiling-process simulation. The main difficulty is that, without assist coiling, the strip head can roll together with the roller and make contact analysis between different layers of the strip under the coiling-process. This article solves such a problem through jointing the strip head and roller by fixed contact for geometric modeling. The material parameters of the strip are listed in Table 1:

Tab. 1 - Material parameters

Material parameter	Value
Roller's modulus of elasticity(GPa)	210
Strip's modulus of elasticity(GPa)	206
Resistance to deformation of Strip(MPa)	280
Strip's tangent modulus(MPa)	1800

A reasonable gridding size is the key point to improve solving accuracy and ensure solving efficiency. The roller and strip are both hexahedron, which is a solid element for gridding. Unit solid64 for the roller is used as a solid element for three-dimensional explicit structure, which consists of 8 nodes with support to all the approved non-linear problems. Unit shell163 for the strip is a shell unit with a 4-node explicit structure. It has a bending and film feature, and can be added with plane loading and normal loading. Such a unit supports all non-linear characteristics for explicit dynamic analysis. To ensure accuracy, the gridding of the strip should be substantially smaller. The ideal gridding size should be as near to a length-width-thickness ratio of 1:1:1 as possible, but the strip in such a model always has a bigger width-thickness ratio, to guarantee that the computing model avoids the bigger size, which would reduce its quality while gridding. Furthermore, to ensure jointing between the strip head and roller by fixed contact, the grids of the strip head should be matched with those of the roller. This benefits the implementation of the constraint in fixed contact. In the case of analyzing the effect of plastic deformation of a strip due to a local high point value, simplifying the width directions of the strip and roller, but setting up the model of ridge-buckle scale, can help reduce the number of units and save computing time.
There are more than 50 methods of contact analysis in the DYNA finite element software, not only for solving the contact problems [14-15] as flexible body - flexible body, flexible body - rigid body and rigid body - rigid body, but also for analyzing elements such as static and dynamic friction, fixed-contact failure of a surface in contact, and the interface between the fluid and solid. As the roller was set as a rigid roller in this article, the flexible body - rigid body contact in a surface - surface contact method is used. Moreover, while coiling the second circle even further, contact between the surfaces of the strip shall be set with the flexible body - flexible body contact method. The contact algorithm includes the dynamic constraint method, penalty function method and distribution parameter method. While the program defines the contact surface, the contact algorithm uses auto generation [16,17].

According to the above introduction, the finite element model can be set up following Fig. 12. In such a model, the effects for strip deformation caused by the local high point sizes on strips were considered. The main size of the model is given in Table 2. The model takes the angular velocity of rotation motion on the roller, and brings coiling tension on the strip end.

Tab. 2 - Main size parameter of model

Size parameter	Value
Roller's outer/ inner diameter (mm)	508/460
Strip width(mm)	1230
Strip thickness(mm)	0.4~0.6
Tension being set(kN)	20~40

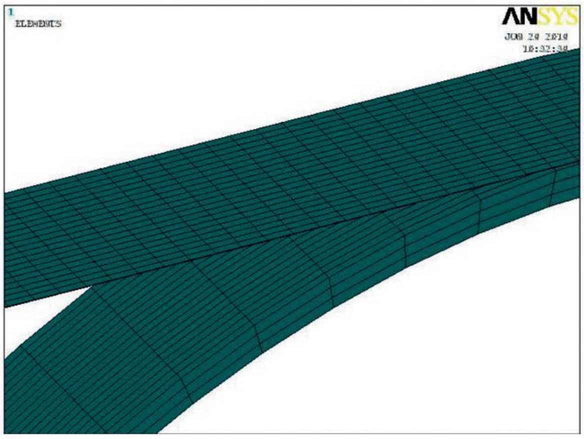

Fig. 12 - Finite element model

Computing result for finite element model

After setting the load step, defining the constraint and load for the finite element, the K file that the LS_DYNA solver needs and makes analysis with. Fig. 13 shows the strip equivalent effective stress in emulation, as shown in the nephogram.

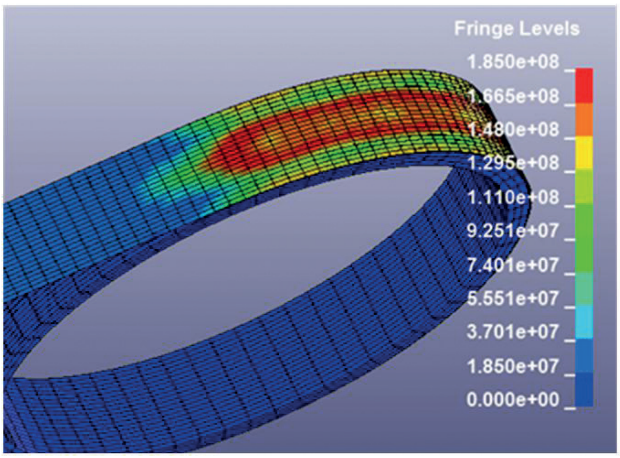

Fig. 13 - Strip coiling equivalent effective stress nephogram

As Fig. 14 shows, strip longitudinal strain capacity near the local high point can reveal that the effect of the local high point is limited to just a small scale on and near the high point. Because of bulging at the local high point of the strip, there is additional strain at the high point when the strip undergoes the coiling process. Alternatively, the radial thrust at the high point of a strip is higher than at its other parts, thus causing the bigger longitudinal fiber strain capacity of a strip at its local high point.

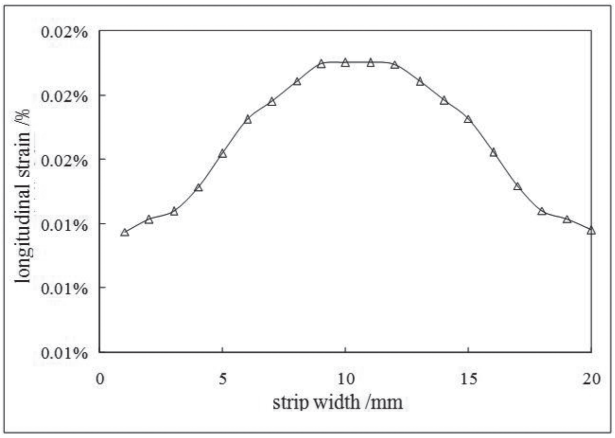

Fig. 14 - Longitudinal strain (Lateral axis = strip with vertical axis = longitudinal strain.)

In Fig. 15, the local high point varies in status, along with the increasing strip coiling circles. The strip thickness is 0.5 mm, the local high point values are 2μm and 3μm, roll diameter is 508mm and coiling tension is 25kN. Fig. 15 shows that the variation of local high points is not raised in proportion with increasing coiling layer number. The first two circles were raised in proportion appropriately, while at the 4th circle the increment rate declined and reached the maximum strip strain value for the layer number concerned. The rate did not increase any longer, and judging by the increasing of the coiling layer number, the increment of strip strain is above 0.02%.

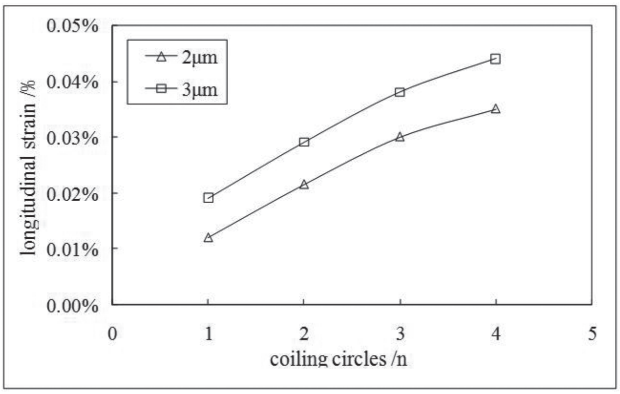

Fig. 15 - Coiling circles against strip strain (Lateral axis= coiling layer number; Vertical axis= longitudinal strain.)

Fig. 16 shows the deformation status for strip thicknesses of 0.4 mm, 0.5 mm and 0.6 mm, a coiling tension of 25kN, and a roll diameter of 508mm; coiling at different local high points. It can be seen that strip longitudinal strain capacity varies in an approximately exponential increase with increased local high point value. The thicker strip has a greater strain capacity against increasing local high point values. Considering the influence of the coiling layer number, the longitudinal strain capacity shall continue to be increased accordingly. For a strain curve while a material is yielding, a 0.5mm thick strip can be taken as an example: the local plastic deformation will occur under coiling when the local high point reaches the value at 6μm.

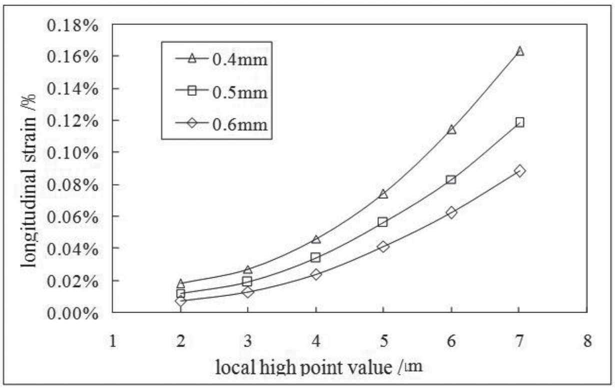

Fig. 16 - Strip strain against different local high points (Lateral axis = local high point value/μm; Vertical axis = increment of strip longitudinal strain capacity)

In Fig. 17, the strip thickness is 0.5; the local high points are 2μm, 3μm, 4μm, and the strip longitudinal strain capacity varies along with the changing coiling tension. It can be seen that the increasing amplitude strain capacity for the strip is not very large while coiling tension changes.

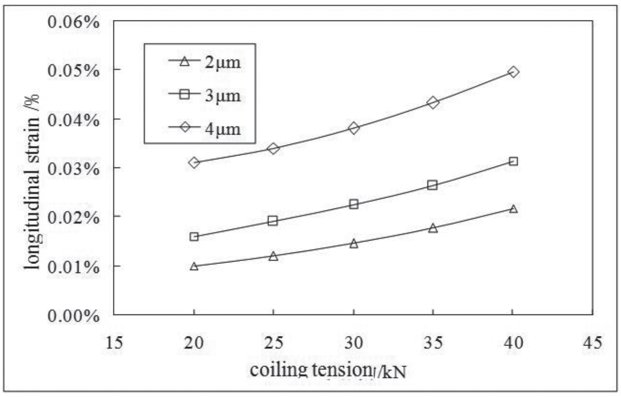

Fig. 17 - Coiling tension against longitudinal strain (Lateral axis = Coiling tension/ kN; Vertical axis = increments of strip longitudinal strain capacity)

CONCLUSION

(1) Based on the fundamental theory of elastic mechanics, the deformation under stress of a strip during the coiling process was analyzed. A computing formula was then derived for the inner layer pressure of a strip during the coiling process, and the relationship between the local high point and ridge buckle was computed.

(2) The three-dimensional finite element model was set. This displayed how the local high point in a strip can truly reflect the real deformation of a strip under the stress of the coiling process.

(3) The variation of local high points in the coiling process was analyzed, along with the strip strain capacity under different local high points and tension. This resulted in a control range of local high points against different strip thicknesses.

(4) The results showed that local plastic deformation can be reduced by controlling the range of local high points against different strip thicknesses. It was also found that the forming mechanism of secondary local curling was due to ridge buckle stress superposition during the coiling process. This provided the theoretical and data support for a control on local curling and ridging in high-precision cold-rolled thin strip.

ACKNOWLEDGEMENTS

This work is supported by Doctoral Program Foundation of Institutions of Higher Education of China (No. 20130006120024) and National Natural Science Funds of China (51404021).

REFERENCES

[1] BAI Zhenhua - The core technology mathematics model for high-speed production of cold continuous rolling machine, China Machine Press, (2009) 28-32.

[2] Melfo W M, Dippenaar R J, Carter CD. Ridge-buckle defect in thin-rolled steel strip, Iron Steel Technol, 3(2006) 54-61.

[3] H.T.Zhu. Effect of hot coil profile containing ridges on ridge-buckle defects of cold rolled thin strip, International Journal of Material Forming , 3 (2010) 21-27.

[4] Melfo W M, Dippenaar R J.Ridges in Hot-Rolled Strip: Microstructural Development as a Function of Temperature Variations in the strip, AISTech Proc, Charlotte, (2005) 295-306.

[5] Melfo W M.Analysis of hot rolling events that lead to ridge-buckle defect in steel strips, University of Wollongong (2006).

[6] BAI Zhenhua, LI Xingdong et al - The influence that local wave shape brings to cold-rolled coiling strip ridge-buckle, Mechanical Engineering Academic Journal, 42(2006) 229-232.

[7] Ovesy H R, Ghannadpour S A M, Zia-Dehkordi E, et al. Buckling analysis of moderately thick composite plates and plate structures using an exact finite strip, Composite Structures, 95(2013) 697-704.

[8] Ghannadpour S A M, Ovesy H R, Zia-Dehkordi E. Buckling and post-buckling behaviour of moderately thick plates using an exact finite strip, Computers and Structures, 147(2015) 172-180.

[9] Bush A, Nicholls R, Tunstal J. Stress levels for elastic buckling of rolled strip and plate, Ironmaking and Steelmaking, 28(2001) 481-484.

[10] Fischer F D, Rammerstorfer F G, Friedl N. Residual stress-induced center wave buckling of rolled strip metal, Journal of applied mechanics, 70(2003) 84-90.

[11] Rammerstorfer F G, Fischer F D, Friedl N. Buckling of free infinite strips under residual stresses and global tension, Journal of applied mechanics, 68(2001) 399-404.

[12] WANG Yong-qin. Modeling of Stress Distribution During Strip Coiling Process, JOURNAL OF IRON AND STEEL RESEARCH, INTERNATIONAL, 19(2012) 06-11

[13] WANG Yidong, YU Bin et al - Local high point's influence for additional wave shape of cold rolled coiling strip. Iron and Steel, (2010) 45-48.

[14] Y.J.Jung, G.T.Lee, C.G.Kang. Coupled thermal deformation analysis considering strip tension and with/without strip crown in coiling process of cold rolled strip. Journal of Materials Processing Technology 131 (2002) 195-201.

[15] Abdelkhalek S, Montmitonnet P, Legrand N, et al. Coupled approach for flatness prediction in cold rolling of thin strip, International Journal of Mechanical Sciences, 53(2011) 661-665.

[16] T. Hatzenbichler, B. Buchmayr, O. Harrer, F. Planitzer. Effect of different contact formulations used in commercial FEM software packages on the results of hot forging simulations, La Metallurgia Italiana, 11(2010) 11-15.

[17] Shang Sucheng, Zhou Hao, Chang Xue, Liu Mingxing, LI Na, Shang Qingqing. Analysis on the structure transformation of landing craft, Mathematical Modelling and Engineering, 1(2014) 11-14.